THE UNIVERSITY OF TEXAS AT DALLAS
McDermott Library

TREASURES
@UT Dallas

School of Natural Sciences and Mathematics

Influence of Dy^{3+} and Tb^{3+} Doping on ^{13}C Dynamic Nuclear Polarization

UT Dallas Author(s):

Peter Niedbalski
Christopher Parish
Andhika Kiswandhi
André Martins
A. Dean Sherry
Lloyd Lumata

Rights:

©2017 American Institute of Physics. This article may be downloaded for personal use only. Any other use requires prior permission of the author and AIP Publishing.

Citation:

Niedbalski, P., C. Parish, A. Kiswandhi, L. Fidelino, et al. 2017. "Influence of Dy^{3+} and Tb^{3+} doping on ^{13}C dynamic nuclear polarization." Journal of Chemical Physics 146(1), doi:10.1063/1.4973317

This document is being made freely available by the Eugene McDermott Library of the University of Texas at Dallas with permission of the copyright owner. All rights are reserved under United States copyright law unless specified otherwise.

Influence of Dy^{3+} and Tb^{3+} doping on ^{13}C dynamic nuclear polarization

Peter Niedbalski,[1] Christopher Parish,[1] Andhika Kiswandhi,[1] Leila Fidelino,[2] Chalermchai Khemtong,[2] Zahra Hayati,[3] Likai Song,[3] André Martins,[2,4] A. Dean Sherry,[2,4] and Lloyd Lumata[1,a)]

[1]*Department of Physics, University of Texas at Dallas, 800 West Campbell Road, Richardson, Texas 75080, USA*
[2]*Advanced Imaging Research Center, University of Texas Southwestern Medical Center, 5323 Harry Hines Boulevard, Dallas, Texas 75390, USA*
[3]*National High Magnetic Field Laboratory, Florida State University, Tallahassee, Florida 32310, USA*
[4]*Department of Chemistry, University of Texas at Dallas, 800 West Campbell Road, Richardson, Texas 75080, USA*

(Received 26 October 2016; accepted 14 December 2016; published online 3 January 2017)

Dynamic nuclear polarization (DNP) is a technique that uses a microwave-driven transfer of high spin alignment from electrons to nuclear spins. This is most effective at low temperature and high magnetic field, and with the invention of the dissolution method, the amplified nuclear magnetic resonance (NMR) signals in the frozen state in DNP can be harnessed in the liquid-state at physiologically acceptable temperature for *in vitro* and *in vivo* metabolic studies. A current optimization practice in dissolution DNP is to dope the sample with trace amounts of lanthanides such as Gd^{3+} or Ho^{3+}, which further improves the polarization. While Gd^{3+} and Ho^{3+} have been optimized for use in dissolution DNP, other lanthanides have not been exhaustively studied for use in ^{13}C DNP applications. In this work, two additional lanthanides with relatively high magnetic moments, Dy^{3+} and Tb^{3+}, were extensively optimized and tested as doping additives for ^{13}C DNP at 3.35 T and 1.2 K. We have found that both of these lanthanides are also beneficial additives, to a varying degree, for ^{13}C DNP. The optimal concentrations of Dy^{3+} (1.5 mM) and Tb^{3+} (0.25 mM) for ^{13}C DNP were found to be less than that of Gd^{3+} (2 mM). W-band electron paramagnetic resonance shows that these enhancements due to Dy^{3+} and Tb^{3+} doping are accompanied by shortening of electron T_1 of trityl OX063 free radical. Furthermore, when dissolution was employed, Tb^{3+}-doped samples were found to have similar liquid-state ^{13}C NMR signal enhancements compared to samples doped with Gd^{3+}, and both Tb^{3+} and Dy^{3+} had a negligible liquid-state nuclear T_1 shortening effect which contrasts with the significant reduction in T_1 when using Gd^{3+}. Our results show that Dy^{3+} doping and Tb^{3+} doping have a beneficial impact on ^{13}C DNP both in the solid and liquid states, and that Tb^{3+} in particular could be used as a potential alternative to Gd^{3+} in ^{13}C dissolution DNP experiments. *Published by AIP Publishing.* [http://dx.doi.org/10.1063/1.4973317]

I. INTRODUCTION

Nuclear magnetic resonance (NMR) spectroscopy, especially of nuclei other than proton and at low concentrations, can be a challenging measurement owing to the inherently weak magnetic moments of nuclear spins.[1] As a result of relatively low gyromagnetic ratio γ of nuclear spins, the spin population difference between Zeeman energy states, quantified by the polarization, can be quite miniscule. This is particularly prominent in the case for low-γ nuclei such as ^{13}C or ^{15}N. Consequently, NMR under these conditions often requires a large number of scans in order to achieve adequate signal-to-noise. While NMR is relatively insensitive, electron paramagnetic resonance (EPR), a similar technology, does not suffer from this problem. This is a consequence of the relatively higher strength of the electron magnetic moment which is 3–4 orders of magnitude stronger than that of most nuclei. Thus, at similar magnetic fields and temperatures, EPR will have a significantly greater polarization, and hence, higher signal strength than NMR.[2]

Dynamic nuclear polarization (DNP) resolves the insensitivity problem of NMR by transferring the high thermal polarization of electrons to nuclei.[3] DNP was originally proposed as a method of increasing polarization in metals,[4] but was quickly expanded to diamagnetic solids.[5–7] The DNP process involves microwave irradiation of a sample of nuclear spins in a glassy solid doped with paramagnetic agents.[3] For most of its history, this technique was used to prepare polarized targets in particle physics experiments,[8] but has been revolutionized for chemical and biomedical applications with the invention of dissolution DNP in 2003.[9] In dissolution DNP, nuclear spins are polarized in the solid state and subsequently dissolved rapidly, resulting in a "hyperpolarized" room-temperature liquid yielding liquid-state signal enhancements of typically more than 10 000-fold.[9,10] Using this technology, samples containing low-γ nuclei such as ^{13}C may be both highly polarized and physiologically compatible, allowing for biomedical applications such as ^{13}C metabolic imaging in real-time.[11–15]

a)Author to whom correspondence should be addressed. Electronic mail: lloyd.lumata@utdallas.edu

The efficiency of DNP is highly dependent on the sample composition and physical conditions under which it takes place. Most commonly, high magnetic fields (typically >3 T) and low temperatures (close to 1 K) are used in order to ensure nearly complete electron polarization. Additionally, the DNP enhancement is contingent on the frequency of microwave irradiation used, which changes based on magnetic field and sample composition. One of the most important determining factors of the overall DNP signal enhancement is sample composition. The free radical used, the nuclei to be polarized, the substrate containing the nuclei, and the solvent in which the nuclei and free radical are dissolved all play an important role in the optimization of DNP. In dissolution DNP, organic free radicals including trityls and nitroxides are most commonly used as the polarizing agents.[16,17] Other radicals such as BDPA,[18] DPPH,[19] and galvinoxyl[20] have been used with some success as well as novel methods such as photoinduced radicals[21] and paramagnetic centers within nanoparticles.[22,23] Nitroxide free radicals have relatively wide EPR linewidths, which are better suited for DNP of high-γ nuclei such as ^{1}H spins and also provide decent polarization levels for low-γ nuclei such as ^{13}C.[24] This class of free radicals maintain their popularity by being comparatively inexpensive, highly water soluble, easily scavenged, and effective for cross polarization DNP.[25–30] Additionally, the DNP efficiency of these radicals may be increased through other means such as deuteration of the glassing matrix.[31–33] Meanwhile, the trityls, particularly OX063, which have some of the narrowest EPR linewidths among free radicals, were found to be excellent polarizing agents for low-γ nuclei like ^{13}C.[16,34] When using these radicals, DNP enhancements may be improved further by the addition of trace amounts of gadolinium.[34–37] Recently, it was found that the addition of holmium to a trityl-doped sample results in liquid state enhancement similar to that achieved by using gadolinium.[38] While the use of these lanthanides may lead to significant polarization gains, the free ion form of these lanthanides may lead to greater toxicity of the DNP sample, which must be considered prior to *in vivo* biomedical application.[39] One method used to combat the toxicity of rare earth metals is to encage these lanthanide ions with a chelating agent, thus rendering them relatively inert in the body.[40] Among the more prominent ligands used in gadolinium contrast agents are DTPA,[40,41] HP-DO3A,[42,43] and DOTA.[44] Of these, DOTA is considered to have high thermodynamic stability and kinetic inertness, and as such is an ideal gadolinium chelating ligand for use in *in vivo* studies.[41]

While a variety of Ln(III) complexes have numerous biomedical applications, particularly in contrast-enhanced MRI,[45] only Gd^{3+} and Ho^{3+} have been studied extensively as beneficial doping agents in ^{13}C dissolution DNP.[35–38] This in part takes precedent from a previous preliminary study which has shown that only Gd^{3+} and Ho^{3+} ions have beneficial effects on ^{13}C DNP, while the other Ln(III) ions appear to have no apparent effect on ^{13}C DNP enhancements for trityl-doped samples.[37] We would like to note that the measurements in the aforementioned previous DNP study on using lanthanide ions[37] were not really extensively optimized in terms of concentration dependence and the fact that the optimum DNP microwave frequency could shift with lanthanide doping. Thus, in this work, we have revisited the question on whether Gd^{3+} and Ho^{3+} really stand alone among the lanthanides as beneficial additives in ^{13}C dissolution DNP samples. Due to the high cost of trityl OX063 free radical and DNP instrumental operation, we have selected only two lanthanides, Tb^{3+} and Dy^{3+}, for extensive ^{13}C DNP optimization studies. Tb^{3+} and Dy^{3+} have among the highest magnetic moments in the lanthanide series, on par with Gd^{3+} and Ho^{3+}. In fact, in terms of magnetic susceptibility (μ_{eff}) that is affected by many other physical properties mostly related to the ion anisotropy, Tb^{3+} and Dy^{3+} presented the highest and most promising parameters.[46] We have used Tb-DOTA and Dy-DOTA for the ^{13}C DNP study and carefully recorded the effects on DNP microwave sweeps, relative ^{13}C solid-state polarization buildup curves, liquid-state ^{13}C enhancement, and relaxation. The substrate used in these studies was [1-^{13}C] sodium acetate, which was chosen for its biological relevance and comparatively low cost. Furthermore, W-band EPR was used to elucidate the physical mechanisms of free electrons that are at play in ^{13}C DNP. With these optimized steps for measurements, the main goal of this work was to investigate whether these two selected lanthanides have any beneficial impact on ^{13}C DNP similar to the effects of Gd^{3+} and Ho^{3+} complexes.

II. EXPERIMENTAL

A. Sample preparation

Chemicals and reagents were acquired commercially and used without further purification. For each sample studied by DNP, 24.9 mg of [1-^{13}C] sodium acetate (Cambridge Isotope Lab, MA) was added to 100 μl of 1:1 v/v water:glycerol solution. This was prepared several hours prior to polarization and frozen at −20 °C until the experiment time. Immediately prior to the polarization, samples were thawed and 2.14 mg of trityl OX063 free radical was added to the solution. The final concentration in the solutions of sodium acetate and trityl OX063 was 3M and 15 mM, respectively. These DNP samples were prepared in 100 μl aliquots and doped with varying concentrations of Dy^{3+}-DOTA or Tb^{3+}-DOTA. The Dy-doped samples were prepared from an aqueous stock solution of 135.0 mM Dy^{3+}-DOTA (deionized water, pH 7.2) and Tb-doped samples from an aqueous stock solution of 124.5 mM Tb^{3+}-DOTA (deionized water, pH 7.2).

The Dy^{3+}-DOTA or Tb^{3+}-DOTA was prepared by adding to solutions free ligand ($DOTA^{4-}$) at M/l molar ratios of 1:1.05, and the resulting solutions were heated at 338 K under stirring for a least 12 h. The pH was kept close to 7 by periodic addition of aqueous KOH. The absence of free Dy^{3+} and Tb^{3+} ions in solution was verified by the xylenol orange test.[47,48] Final concentrations were checked by the Evans method.

The concentrations studied for Dy were 1.0, 1.5, 2.0, 3.0, and 4.0 mM and for Tb were 0.125, 0.25, 0.5, 1.0, 1.5, 2.0, 3.0, and 4.0 mM. Control samples and two additional samples, one containing 2 mM Ho^{3+}-DOTA and one containing 2 mM Gd^{3+}-DOTA, were also made for comparison. The holmium and gadolinium samples were prepared from aqueous stock solutions of 218 mM Ho^{3+}-DOTA (deionized water, pH 7.2) and 79.65 mM Gd^{3+}-DOTA (deionized water, pH 7.2),

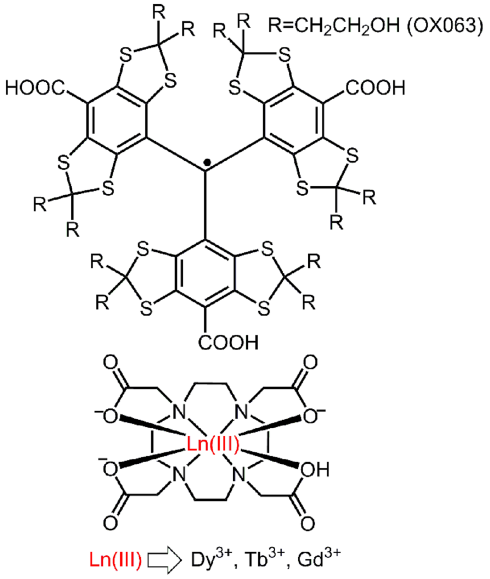

FIG. 1. The free radical polarizing agent and lanthanides complexes used in this work.

respectively. The free radical and DOTA ligand used in this work may be seen in Fig. 1.

B. EPR measurements

EPR measurements were conducted on a reference sample as well as samples doped with Tb, Gd, and Dy. The EPR experiments were performed prior to DNP experiments, and as such optimal concentrations had not yet been determined. Previous work has shown that the optimal concentration for both gadolinium and holmium is 2 mM,[34,35,38] so this was chosen to be the concentration of terbium and dysprosium studied in order to compare their electron T_1 under the same conditions. Measurements were performed at the National High Magnetic Field Laboratory (NHMFL) in Tallahassee, FL in the W-band (94 GHz) on a Bruker E680 EPR spectrometer (Bruker Biospin, Billerica, MA) using a Bruker TE_{011} cylindrical cavity. The temperature of the sample was regulated using a CF1200 helium flow cryostat (Oxford Instruments, UK). Prior to insertion in the cylindrical cavity, samples were loaded in 0.15 mm ID thin quartz capillary tubes. Temperature dependent electronic T_1 data for trityl OX063 were recorded using saturation recovery, and the EPR spectra were monitored using the field-swept electron spin-echo method. Samples were studied at temperatures down to the low temperature limit of 5 K in order to most closely match DNP conditions.

C. Hyperpolarization and NMR measurements

All hyperpolarization experiments were conducted at the Advanced Imaging Research Center at the University of Texas Southwestern Medical Center (UTSW) using the commercial HyperSense polarizer (Oxford Instruments, UK). This polarizer uses a 3.35 T superconducting magnet, and the cryostat vacuum space has a base temperature of 1.2 K due to a roots blower pump vacuum system (Edwards Vacuum, UK). Irradiation of the sample in this polarizer is provided by a 100 mW ELVA microwave source (ELVA-1 millimeter Wave Division, RU) with a 400 MHz sweepable frequency range.

^{13}C samples prepared as described above were inserted into the polarizer. Before running polarizing buildup experiments, microwave frequency sweeps were conducted for samples with various concentrations of Tb^{3+} and Dy^{3+} in order to determine the optimum polarization frequencies for DNP. The ^{13}C NMR signal of the sample was measured after 3 min of polarization at 5 MHz intervals over the range of the microwave source using a sweep program in the HyperSense. After each NMR scan, a series of hard pulses was applied to the sample to remove polarization built up at the previous frequency. In this manner, the positive P(+) and negative P(−) polarization peaks were found for different concentrations of the studied lanthanides. These were then normalized for comparison.

After the optimum irradiation frequencies were found, ^{13}C polarization buildup curves were measured for each sample. This was accomplished by irradiating each sample at the frequency determined by the positive polarization peak P(+) and measuring the ^{13}C NMR signal every 3 min until the curve had approximately reached a plateau. The actual percent polarization for samples was not found due to the prohibitively long acquisition times necessary to measure the thermal ^{13}C polarization. Rather, the relative polarization level was used to evaluate the efficacy of the lanthanide complexes on ^{13}C DNP. This is in line with previous studies which have used the same method to compare DNP performance.[32,35–38] Build-up curves were recorded and fit with single exponential equations, and using the fit, the relative polarization at 10 000 s was extrapolated.

Due to the large number of samples to be studied and limited access to the HyperSense polarizer, only single build-up curves were taken for samples with non-optimal concentrations of lanthanide. Meanwhile, the ^{13}C DNP samples doped with optimal lanthanide concentrations 1.5 mM Dy^{3+}-DOTA, 0.25 mM Tb^{3+}-DOTA, 2 mM Gd^{3+}-DOTA, and the control sample were each measured in triplicate. For each of the three trials, new samples were freshly made prior to polarization. One dissolution per lanthanide was carried out after these samples had reached maximum polarization. Upon dissolution, approximately 4 ml of aqueous solution of hyperpolarized [1-^{13}C] acetate was transferred through 0.125 in. OD PTFE tubing to a 10 mm NMR tube (Wilmad-LabGlass, NJ) which was already placed inside a 400 MHz Varian NMR magnet (Agilent Technologies, CA). This transfer was an automated process with a total shuttling time of 8 s from the HyperSense to the high resolution NMR magnet. Once the liquid had been transferred, the decay of the hyperpolarized signal was monitored by applying 5° RF pulses at 2 s intervals. The first scan was taken immediately following the transfer of hyperpolarized liquid with a delay of 0.01 s. Following the array of scans, the sample was removed from the magnet for a specific time to ensure complete relaxation of the hyperpolarized signal. Subsequently, it was then returned to the magnet where a single NMR scan was taken using a 90° RF pulse in order to obtain the thermal equilibrium polarization from which liquid-state enhancements could be calculated.

D. Data analysis

All data were plotted and analyzed using Igor Pro version 6.2 (Wavemetrics, Lake Oswego, OR). Mean values and standard deviations were calculated for experiments with $N = 3$ trials. Liquid-state ^{13}C NMR data taken post dissolution in a Varian NMR spectrometer were processed using ACD labs version 12.0 (Advanced Chemistry Development, Toronto, Canada).

III. RESULTS AND DISCUSSION

One of the primary determining factors in total DNP enhancement of the NMR signal is the free radical that provides the electrons from which polarization is transferred to nuclei.[17,18,20,21,31,34,49] Trityl OX063, the stable organic radical used in this work, has a very narrow EPR linewidth that makes it ideal for polarizing low-γ nuclei such as ^{13}C. When using this free radical to polarize low-γ nuclei such as ^{13}C spins, DNP data at 3.35 T and temperatures close to 1 K have shown indications of thermal mixing (TM) as the predominant DNP mechanism.[24,50–53] Other DNP data at similar conditions suggested that the mechanism could be a combination of the solid effect (SE) and cross effect (CE).[54–56] Unlike the solid effect (SE)[57] and the cross effect (CE),[54,58] TM is a many-spin model for polarization that treats spin interactions as thermodynamic reservoirs.[24,59] Namely, these reservoirs are the nuclear Zeeman system (NZS) and electron Zeeman system (EZS), and the electron dipolar system (EDS). In terms of this model, the polarization method may be qualitatively understood as microwave irradiation cooling the EDS and subsequent thermal contact with the NZS (via the hyperfine interaction), leading to a decrease in the NZS spin temperature, i.e., an increase in nuclear polarization. Quantitatively, the maximum polarization achievable in this model is

$$P_{max} = \mathscr{B}_I\left(I\beta_L\omega_e\frac{\omega_I}{2D}\frac{1}{\sqrt{\eta\,(1+f\,)}}\right), \tag{1}$$

where $\mathscr{B}_I$ is the Brillouin function, I the nuclear spin, $\beta_L = \hbar/kT_L$ the inverse lattice temperature, ω_e and ω_I the electron and nuclear Larmor frequencies, respectively, D the radical EPR linewidth, $\eta = t_Z/t_D$ the ratio of electron Zeeman to electron dipolar relaxation times, and f a general "leakage factor" that encompasses nuclear relaxation effects.[24]

A. EPR of trityl doped with Ln^{3+}

Because the free radical plays such a significant role in determining the overall polarization enhancement, it stands to reason that changing the electronic properties of the radical by addition of lanthanide complexes could change the maximum polarization.[34,60] In order to thoroughly investigate these changes, field swept EPR spectra (Fig. 2(a)) and the temperature dependence of electron T_1 were studied for the samples of interest. T_1 was determined by fitting the electron relaxation recovery curves using a double-exponential build-up $M(t) = M_a\exp(-t/T_{1,a}) + M_b\exp(-t/T_{1,b}) + C$. This equation resultsin two relaxation times, the longer of which ($T_{1,a}$)

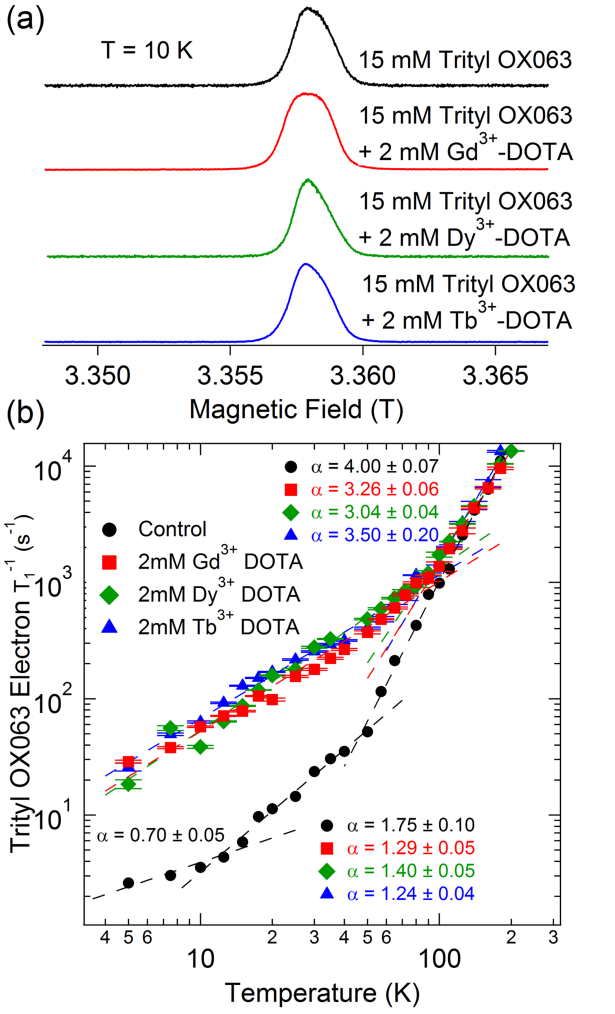

FIG. 2. (a) Field-swept W-band EPR spectra of trityl OX063 at 10 K in the absence or presence of trace amounts of lanthanides. (b) Temperature dependence of electron T_1 for trityl OX063 with and without lanthanide doping. The power law equation of best fit is shown for each data set with dashed lines and the power displayed for each sample.

corresponds to the electron T_1 while the shorter corresponds to the relaxation effects contributed by electron-electron cross relaxation effects.[61,62] Electron T_1^{-1} was plotted vs. temperature on a log-log plot (Fig. 2(b)), and a power law equation ($T_1^{-1} = AT^{\alpha}$) was fitted to the data.

At high temperatures, the electron T_1 of undoped trityl OX063 increases rapidly as the temperature is reduced, with a dependence of $\alpha \approx 4$. This suggests that at temperatures above about 50 K, electron relaxation is dominated by multiple-phonon processes such as the Orbach process.[63] Below 50 K to about 20 K, there is a decrease in the rate of change of T_1^{-1}, with temperature having $\alpha \approx 1.75$. Because this value is close to 2, it indicates that electron relaxation in this temperature regime is dominated by the Raman process.[63] Below 20 K, the dependence falls to $\alpha \approx 0.70$, which points to the one-phonon direct process as the primary means of electron relaxation.[63]

Samples doped with 2 mM Ln(III) complex gave nearly identical electron relaxation data. For each of the samples, there was only one major change in the power law fitting, which occurred at a higher temperature (90 K) than did

the shift in the reference data. Above 90 K, the electron relaxation rate is nearly identical to that of the reference sample, but is much more rapid below this temperature. In this low temperature regime, T_1^{-1} changes with temperature with an $\alpha \approx 1$ dependence, suggesting that below 90 K, the direct process dominates the electron relaxation behavior for the lanthanide doped samples. The lowest temperature studied for EPR was 5 K, but based on the trends of both the reference and lanthanide samples, it is likely that electron relaxation is dominated by the direct process at DNP temperatures near 1 K. This is corroborated by a previous study[34] which shows that the trityl electron relaxation of a reference sample close to 1 K falls reasonably close to a fit of relaxation data between 5 and 20 K extrapolated to 1 K.

B. ^{13}C solid state polarization

In order to ensure that samples were irradiated at the optimum frequency, microwave frequency sweeps were taken for all samples. Representative ^{13}C microwave frequency sweeps are shown in Fig. 3. Similar to previous studies of Gd^{3+} in DNP, Tb^{3+} and Dy^{3+} doped samples resulted in DNP spectra that had P(+) and P(−) shifted toward each other.[36,60] At the optimum concentration of Dy^{3+}-DOTA (1.5 mM), both positive and negative polarization peaks were shifted by 20 MHz from the reference sample. This shift was consistent over all concentrations of Dy studied, only increasing to 25 MHz for both peaks with 4 mM Dy. For the sample doped with the optimum concentration of Tb^{3+}-DOTA (0.25 mM), P(+) was shifted by 25 MHz, while P(−) was shifted only by 20 MHz. Decreasing the concentration of Tb^{3+} by half reduced the shift to 15 MHz from reference for both peaks, while increasing the concentration to 4 mM Tb^{3+} increased it to 30 MHz.

From a theoretical perspective, the locations of positive and negative polarization peaks can be approximated by Borghini's spin-temperature model.[3,64] Using this model, the DNP spectrum, including P(+) and P(−), depends almost entirely on the features of the EPR spectrum of the free radical used, with smaller contributions from electron and nuclear relaxation. In order to understand the microwave spectra, it is important to consider the EPR data gathered, which show minimal differences in EPR spectra and very significant differences in electron relaxation as discussed above. Though electron relaxation is a less dominant contributing factor in the microwave spectra based on the original Borghini model, it is possible that the magnitude change in relaxation time at low temperature is sufficient to cause a narrowing of the DNP spectrum.

On the other hand, other works have suggested that DNP under similar experimental conditions may be described by a combination of the solid effect and indirect cross effect that could be prevalent in samples having paramagnetic centers with inhomogeneously broadened EPR line shapes.[54–56] The change in DNP spectrum seen with lanthanide doping may be understood equally well by this model. The shortening of electronic T_1 induced by the lanthanide ion changes the level of contribution from the SE and CE, in this case accentuating the contributions from both mechanisms.[55] It is important to note that full quantum mechanical models have been developed to explain this experimental DNP effect using these 2-spin and 3-spin processes.[54–56]

Once the polarization peaks were determined by way of microwave frequency sweeps, polarization build-up curves were taken by irradiating samples at the positive polarization peak P(+) while monitoring polarization at 3 min intervals. Initially, concentrations of 0 mM, 1 mM, 1.5 mM, 2 mM, 3 mM, and 4 mM of both Dy^{3+} and Tb^{3+} were studied. Samples were polarized for between 1.5 and 2 h and the data fit with a single exponential. For final comparison, data were extrapolated to 10 000 s. After these data were collected, it was found that Dy^{3+} had an optimum concentration of 1.5 mM. In addition, it was found that 0.25 mM Tb^{3+} doping resulted in the largest polarization gain. ^{13}C polarization enhancements relative to the reference sample are displayed in Fig. 4(a) for each of the concentrations of Tb and Dy studied. The polarization increases from 0 mM doping to the optimum concentration and decreases fairly rapidly at concentrations above the optimum. This is in contrast to the behavior of Gd^{3+}, which yields a "plateau" in polarization level improvement at concentrations between 2 and 8 mM,[37,60] but is quite similar to the "peak" behavior exhibited by Ho^{3+} doping.[37,38]

In Fig. 4(b), the build-up time constant is shown for each concentration of the two lanthanides. From these data, it is

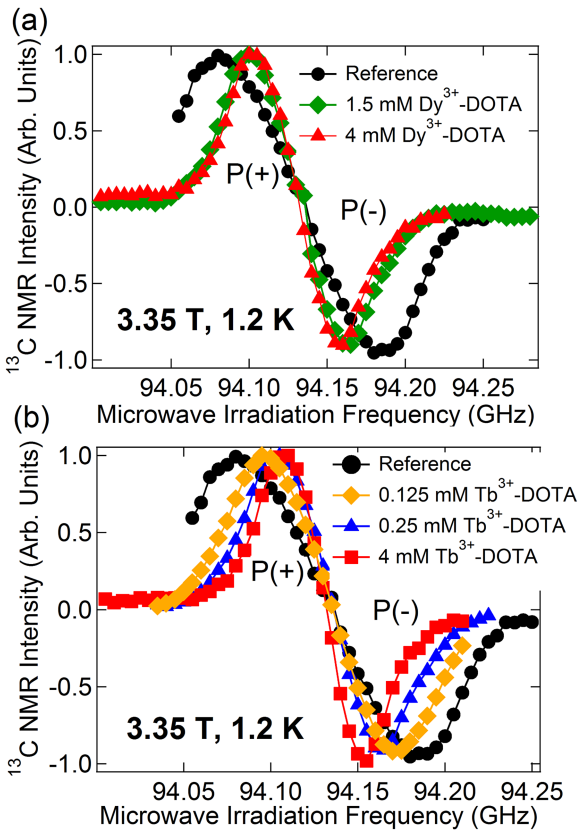

FIG. 3. Microwave frequency sweeps of ^{13}C DNP signals for 100 μl samples of 3M [1-^{13}C] sodium acetate in 1:1 v/v glycerol:water doped with 15 mM trityl OX063 and varying concentrations of (a) Dy-DOTA and (b) Tb-DOTA. All measurements were taken at 3.35 T and 1.2 K with a 100-mW sweepable microwave source.

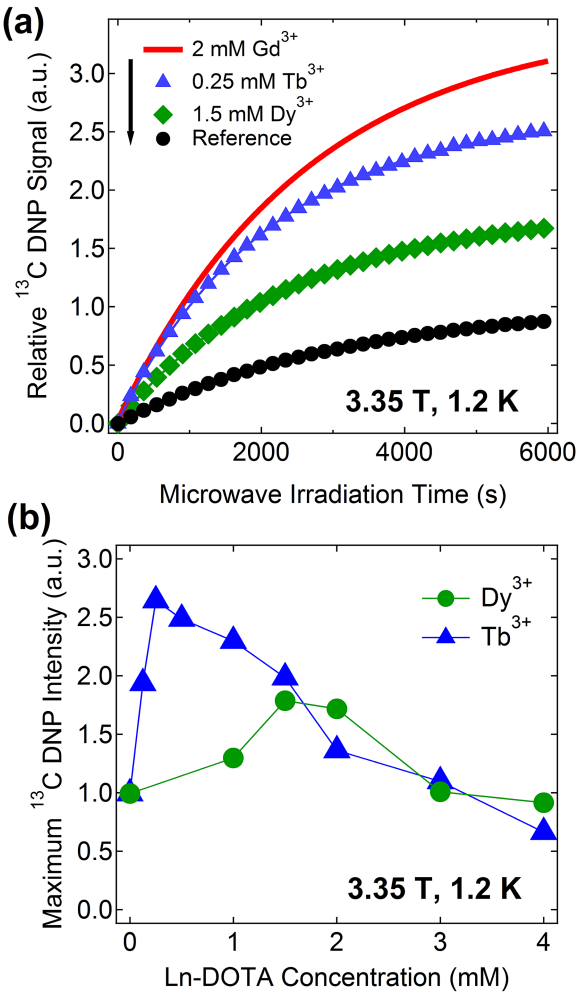

FIG. 4. (a) Relative ^{13}C DNP build-up curves for [1-^{13}C] acetate doped with 15 mM trityl OX063 and doped with the specified amount of Ln(III) complex. (b) The relative ^{13}C DNP enhancement of Tb^{3+}- and Dy^{3+}-doped samples as a function of their concentration. ^{13}C DNP intensities were normalized with respect to the DNP signal of the reference sample.

clear that, generally, a higher concentration of Tb or Dy leads to faster build-up. However, for Tb, even very small concentrations drastically reduce the polarization time, while for Dy, even high concentrations do not increase the polarization rate significantly. ^{13}C polarization build-up curves using optimal concentrations of each of the lanthanides studied are shown in Fig. 4(c). All curves are scaled such that the reference data are normalized. Dy was found to be the least effective of the lanthanides studied with a less than 2-fold enhancement. While ^{13}C DNP samples doping with Tb (~2.5-fold) and Ho (~3-fold) yielded significant improvements in DNP level with respect to that of the reference sample, it is apparent that Gd (~3.5-fold) doping in the sample results in the greatest solid-state ^{13}C polarization gain.

We would like to point out that the improved ^{13}C polarization level observed here with Tb^{3+} and Dy^{3+} doping is a combined result of determining the optimum doping concentration and optimum microwave irradiation frequency. Without carefully following the shifts in optimum microwave frequency with lanthanide doping, the advantage of Tb or Dy doping in ^{13}C DNP may not be as prominent as they were found to be here. For instance, the optimum microwave frequencies for the reference (0 mM Tb-DOTA) and optimally Tb-doped (0.25 mM Tb-DOTA) ^{13}C DNP samples are approximately 25 MHz apart. Without the 25 MHz microwave shift correction for Tb doping, one could look at ^{13}C DNP spectra shown in Fig. 3(b) and predict that the polarization level will only be around 50% of the supposed maximum polarization. Furthermore, the achieved ^{13}C polarization levels are very dependent on the concentration of the lanthanides as can be seen in Fig. 4(b). The ^{13}C DNP enhancement effects of Dy^{3+} and Tb^{3+} doping reported here appear to be at odds with a previous study that showed that except for Gd^{3+} and Ho^{3+}, the other lanthanides including Tb^{3+} and Dy^{3+} had no apparent beneficial impact on ^{13}C DNP.[37] In terms of sample composition, the primary difference between the two studies is the use of Ln^{3+} chlorides by Gordon *et al.*,[37] whereas in this study each lanthanide was chelated in a DOTA complex. It is possible that the ligand to which the lanthanides are bound affects the magnetic properties in such a way as to increase ^{13}C polarization enhancement.[65–67] Moreover, the more probable reason for this difference in the results is that, unlike the aforementioned previous study,[37] the microwave frequency shift and lanthanide concentration dependence were carefully followed in this work.

The improvement of the ^{13}C DNP signal with lanthanide doping is attributed to the shortening of the electronic relaxation time of the free radical through interaction with the lanthanide dopant.[37,60,68] Under the thermal mixing model, this may be seen in Equation (1) in which η is reduced by a shortening of electronic T_1, leading to greater achievable polarization. It should be noted that the improvement of ^{13}C polarization may also be described using a combination of the cross and solid effects as presented by Ravera *et al.*[55] In either case, it is clear that there are a number of factors in addition to electronic T_1 that must contribute given that EPR shows that the trityl electron relaxation rate is similarly affected by each of the lanthanides studied. One possible explanation is the effect of a given lanthanide on the nuclear relaxation rate as discussed previously. Given this, though, it is difficult to pinpoint the origin of the significant polarization differences among the lanthanides. Of the four different lanthanides considered in this work, magnetic moment strength ranges from 7.94 μ_B for Gd^{3+} to 10.6 μ_B for Dy^{3+} and Ho^{3+} with Tb^{3+} intermediate at 9.7 μ_B.[65] Additionally, the electronic relaxation rates for Ho^{3+} and Tb^{3+} are nearly identical at room temperature, with Dy^{3+} having a slightly longer relaxation time and Gd^{3+} a relaxation time four orders of magnitude longer.[69,70] Of course, low temperatures could have a significant effect particularly on the relaxation behavior of lanthanide ions, but these values point to the difficulty of assigning a precise cause for the observed polarization behavior. It is currently unclear to us as to the exact cause of the drastic difference in optimal concentration for Tb^{3+} when compared to the other studied lanthanides. One possibility is that it might be related to the degenerate ground state present for this lanthanide. From all the lanthanides studied here presenting half-odd integer values, Tb^{3+} is the only one not belonging to the family of the Kramers ions. This is associated with non-constant magnetic moments in the absence (or presence) of an external magnetic field.[71,72]

C. Liquid state dissolution

After the optimal concentrations of Tb^{3+} and Dy^{3+} were determined, the liquid state properties of the samples with optimal concentrations were studied by rapidly dissolving the sample and monitoring the ^{13}C NMR signal in a 400 MHz high resolution magnet. We would like to note that the transfer of the dissolution liquid from the 3.35 T hyperpolarizer to the NMR tube in a 9.4 T NMR magnet takes 8 s to complete. All liquid-state ^{13}C NMR enhancements reported here were taken right after the dissolution transfer. In order to compare the liquid state enhancements of the Ln(III) doped samples, T_1 was determined by fitting the relaxation data to an exponential decay as previously described.[50,73] Nuclear relaxation due to both T_1 relaxation and RF pulse excitation was taken into account in this fitting. The data collected monitoring relaxation as well as the fitting is shown in Fig. 5(a). From this, it is clear that Gd^{3+}, despite being chelated in a DOTA complex, still has a significant shortening effect on the ^{13}C T_1 due to its strong paramagnetism.[74] Tb^{3+} and Dy^{3+}, on the other hand, have almost no effect on liquid-state T_1, with relaxation data essentially identical to the reference sample. This may be explained by the very rapid electronic relaxation times of the electrons of these lanthanides, which reduce the overall effect on nuclear relaxation.[37]

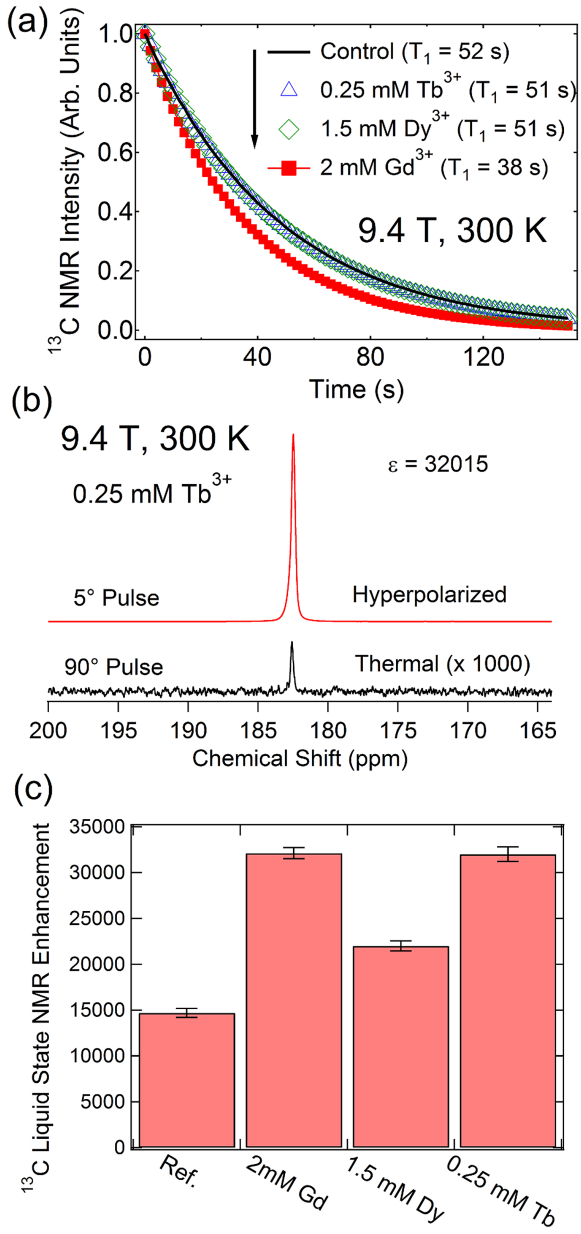

FIG. 5. (a) Decay of NMR signal intensity following dissolution of the polarized sample for a reference sample and samples doped with Tb^{3+}, Dy^{3+}, and Gd^{3+}. (b) Representative figure displaying the hyperpolarized and thermal ^{13}C NMR signal for a Tb^{3+}-doped sample. (c) Comparison of liquid state NMR enhancements for the Ln(III) complexes studied in this work.

In order to quantify the overall liquid state enhancement achieved by each sample, the integrated area under each NMR peak was calculated for both the hyperpolarized (A_{HP}) and thermal (A_{Th}) signals. Then, the DNP enhancement was calculated as documented previously.[38] The hyperpolarized ^{13}C NMR spectra were taken approximately 8 s after the initial dissolution in order to accommodate the shuttling time from the polarizer to NMR magnet. A representative hyperpolarized and thermal signal, taken for the 0.25 mM Tb^{3+} sample, is shown in Fig. 5(b). The enhancements for Tb^{3+}, Dy^{3+}, Gd^{3+}, and the reference sample are shown in Fig. 5(c). Despite a solid state polarization about 3.5 times that of the reference, Gd^{3+} doping results in a liquid state enhancement just over twice that of the reference sample. Significantly, Tb^{3+} results in a nearly identical liquid state enhancement. This is a result of T_1 relaxation in the time interval between polarization and the start of the NMR scan. Because the relaxation rate with Gd^{3+} is increased, there is a greater amount of polarization lost during shuttling than for Tb^{3+} or Dy^{3+}, allowing for comparable liquid state enhancements for Tb^{3+} in spite of significantly lower solid state enhancement. The fact that Dy^{3+} and Tb^{3+} are less efficient relaxation agents compared to Gd^{3+} is advantageous for ^{13}C dissolution DNP since longer nuclear T_1 translates to longer hyperpolarization lifetime of ^{13}C spins.

IV. CONCLUSION

In summary, we have shown that in addition to Gd^{3+} and Ho^{3+} doping, Dy^{3+} and Tb^{3+} complexes are also beneficial additives to samples for ^{13}C DNP at 3.35 T and 1.2 K. Similar to the effects of Gd^{3+} and Ho^{3+} doping, the locations of the optimum microwave irradiation frequencies for ^{13}C samples doped with Dy^{3+} and Tb^{3+} are shifted depending upon the concentration, and thus it is important to carefully follow these shift corrections for optimized DNP results. The optimum concentrations for Tb-DOTA and Dy-DOTA doping were found to be 0.25 mM and 1.5 mM, respectively, which are relatively lower than the optimal DNP concentrations of Gd^{3+} (2 mM) and Ho^{3+} (2 mM) doping. At the optimum concentrations, Dy^{3+} and Tb^{3+} doping yielded significant improvements on the ^{13}C solid-state DNP signals, with enhancement factors of around 1.8 and 2.5-fold, respectively, relative to the ^{13}C DNP signal of a reference or undoped sample. W-band EPR results have shown that while the trityl OX063 free radical spectra are not significantly affected by lanthanide doping, the electron T_1 of the free radical is drastically reduced especially at low temperatures. The significant gain in ^{13}C DNP signal with lanthanide doping is ascribed to a thermal mixing model where shortened electron T_1 of the free radicals leads to dominant

electron cooling in DNP, thus resulting in lower spin temperature in electron dipolar system, and consequently higher nuclear polarization. Moreover, Tb^{3+} and Dy^{3+} are less effective relaxation agents compared to Gd^{3+}—an attribute that is advantageous in preserving the hyperpolarized state after the dissolution process.

ACKNOWLEDGMENTS

The authors would like to acknowledge support from the U.S. Department of Defense (DOD), Grant No. W81XWH-14-1-0048 (L.L.), as well as the Robert A. Welch Foundation, Grant Nos. AT-584 (A.D.S.) and AT-1877 (L.L.). Additionally, the authors acknowledge the NHMFL user collaboration grants program Award No. 5080 (L.S.). EPR was performed at NHMFL, which is supported by the National Science Foundation (NSF) Cooperative Agreement No. DMR 1157490 and the State of Florida. The DNP facility at UTSW is supported by the National Institutes of Health (NIH) Grant No. 8P41-EB015908.

[1] A. Abragam, *The Principles of Nuclear Magnetism* (Clarendon Press, 1961).
[2] M. Brynda, in *Biomedical Applications of Biophysics*, edited by T. Jue (Humana Press, 2010), pp. 59–98.
[3] A. Abragam and M. Goldman, Rep. Prog. Phys. **41**, 395 (1978).
[4] A. W. Overhauser, Phys. Rev. **89**, 689 (1953).
[5] A. Abragam, Phys. Rev. **98**, 1729 (1955).
[6] C. D. Jeffries, Phys. Rev. **106**, 164 (1957).
[7] C. D. Jeffries, *Dynamic Nuclear Orientation* (Interscience Publishers, 1963).
[8] D. G. Crabb and W. Meyer, Annu. Rev. Nucl. Part. Sci. **47**, 67 (1997).
[9] J. H. Ardenkjær-Larsen, B. Fridlund, A. Gram, G. Hansson, L. Hansson, M. H. Lerche, R. Servin, M. Thaning, and K. Golman, Proc. Natl. Acad. Sci. U. S. A. **100**, 10158 (2003).
[10] J. H. Ardenkjaer-Larsen, J. Magn. Reson. **264**, 3 (2016).
[11] T. Prisner and W. Köckenberger, Appl. Magn. Reson. **34**, 213 (2008).
[12] F. A. Gallagher, M. I. Kettunen, and K. M. Brindle, Prog. Nucl. Magn. Reson. Spectrosc. **55**, 285 (2009).
[13] K. M. Brindle, S. E. Bohndiek, F. A. Gallagher, and M. I. Kettunen, Magn. Reson. Med. **66**, 505 (2011).
[14] K. Golman and J. S. Petersson, Acad. Radiol. **13**, 932 (2006).
[15] K. Golman, R. in 't Zandt, and M. Thaning, Proc. Natl. Acad. Sci. U. S. A. **103**, 11270 (2006).
[16] J. H. Ardenkjaer-Larsen, S. Macholl, and H. Jóhannesson, Appl. Magn. Reson. **34**, 509 (2008).
[17] U. L. Günther, in *Modern NMR Methodology*, edited by H. Heise and S. Matthews (Springer, Berlin, Heidelberg, 2011), pp. 23–69.
[18] L. Lumata, S. J. Ratnakar, A. Jindal, M. Merritt, A. Comment, C. Malloy, A. D. Sherry, and Z. Kovacs, Chem. - Eur. J. **17**, 10825 (2011).
[19] L. Lumata, M. Merritt, C. Khemtong, S. J. Ratnakar, J. van Tol, L. Yu, L. Song, and Z. Kovacs, RSC Adv. **2**, 12812 (2012).
[20] L. L. Lumata, M. E. Merritt, C. R. Malloy, A. D. Sherry, J. van Tol, L. Song, and Z. Kovacs, J. Magn. Reson. **227**, 14 (2013).
[21] A. Capozzi, J.-N. Hyacinthe, T. Cheng, T. R. Eichhorn, G. Boero, C. Roussel, J. J. van der Klink, and A. Comment, J. Phys. Chem. C **119**, 22632 (2015).
[22] P. Dutta, G. V. Martinez, and R. J. Gillies, J. Phys. Chem. Lett. **5**, 597 (2014).
[23] M. C. Cassidy, H. R. Chan, B. D. Ross, P. K. Bhattacharya, and C. M. Marcus, Nat. Nanotechnol. **8**, 363 (2013).
[24] J. Heckmann, W. Meyer, E. Radtke, G. Reicherz, and S. Goertz, Phys. Rev. B **74**, 134418 (2006).
[25] S. Jannin, A. Bornet, R. Melzi, and G. Bodenhausen, Chem. Phys. Lett. **549**, 99 (2012).
[26] S. Jannin, A. Comment, F. Kurdzesau, J. A. Konter, P. Hautle, B. van den Brandt, and J. J. van der Klink, J. Chem. Phys. **128**, 241102 (2008).
[27] A. Bornet, R. Melzi, A. J. Perez Linde, P. Hautle, B. van den Brandt, S. Jannin, and G. Bodenhausen, J. Phys. Chem. Lett. **4**, 111 (2013).
[28] M. Batel, M. Krajewski, A. Däpp, A. Hunkeler, B. H. Meier, S. Kozerke, and M. Ernst, Chem. Phys. Lett. **554**, 72 (2012).
[29] M. Batel, M. Krajewski, K. Weiss, O. With, A. Däpp, A. Hunkeler, M. Gimersky, K. P. Pruessmann, P. Boesiger, B. H. Meier, S. Kozerke, and M. Ernst, J. Magn. Reson. **214**, 166 (2012).
[30] B. Vuichoud, J. Milani, A. Bornet, R. Melzi, S. Jannin, and G. Bodenhausen, J. Phys. Chem. B **118**, 1411 (2014).
[31] P. Niedbalski, C. Parish, A. Kiswandhi, and L. Lumata, Magn. Reson. Chem. **54**, 962 (2016).
[32] L. Lumata, M. E. Merritt, and Z. Kovacs, Phys. Chem. Chem. Phys. **15**, 7032 (2013).
[33] F. Kurdzesau, B. van den Brandt, A. Comment, P. Hautle, S. Jannin, J. J. van der Klink, and J. A. Konter, J. Phys. D: Appl. Phys. **41**, 155506 (2008).
[34] L. Lumata, Z. Kovacs, A. D. Sherry, C. Malloy, S. Hill, J. van Tol, L. Yu, L. Song, and M. E. Merritt, Phys. Chem. Chem. Phys. **15**, 9800 (2013).
[35] L. Friesen-Waldner, A. Chen, W. Mander, T. J. Scholl, and C. A. McKenzie, J. Magn. Reson. **223**, 85 (2012).
[36] A. Kiswandhi, B. Lama, P. Niedbalski, M. Goderya, J. Long, and L. Lumata, RSC Adv. **6**, 38855 (2016).
[37] J. W. Gordon, S. B. Fain, and I. J. Rowland, Magn. Reson. Med. **68**, 1949 (2012).
[38] A. Kiswandhi, P. Niedbalski, C. Parish, P. Kaur, A. Martins, L. Fidelino, C. Khemtong, L. Song, A. D. Sherry, and L. Lumata, Phys. Chem. Chem. Phys. **18**, 21351 (2016).
[39] K. T. Rim, K. H. Koo, and J. S. Park, Saf. Health Work **4**, 12 (2013).
[40] X. Wang, T. Jin, V. Comblin, A. Lopez-Mut, E. Merciny, and J. F. Desreux, Inorg. Chem. **31**, 1095 (1992).
[41] L. D. Leon-Rodriguez and Z. Kovacs, Bioconjugate Chem. **19**, 391 (2008).
[42] G. W. White, W. A. Gibby, and M. F. Tweedle, Invest. Radiol. **41**, 272 (2006).
[43] K. T. Cheng, Molecular Imaging Contrast Agent Database MICAD, National Center for Biotechnology Information (US), Bethesda, MD, 2004.
[44] D. Meyer, M. Schaefer, and B. Bonnemain, Invest. Radiol. **23**(Suppl 1), S232 (1988).
[45] S. Aime, M. Botta, M. Fasano, and E. Terreno, Chem. Soc. Rev. **27**, 19 (1998).
[46] G. Pintacuda, M. John, X.-C. Su, and G. Otting, Acc. Chem. Res. **40**, 206 (2007).
[47] S. Aime, M. Botta, and G. Ermondi, Inorg. Chem. **31**, 4291 (1992).
[48] A. Barge, G. Cravotto, E. Gianolio, and F. Fedeli, Contrast Media Mol. Imaging **1**, 184 (2006).
[49] M. C. Cassidy, C. Ramanathan, D. G. Cory, J. W. Ager,and C. M. Marcus, Phys. Rev. B **87**, 161306 (2013).
[50] L. Lumata, A. K. Jindal, M. E. Merritt, C. R. Malloy, A. D. Sherry, and Z. Kovacs, J. Am. Chem. Soc. **133**, 8673 (2011).
[51] L. Lumata, M. E. Merritt, C. Malloy, A. D. Sherry, and Z. Kovacs, Appl. Magn. Reson. **43**, 69 (2012).
[52] J. Wolber, F. Ellner, B. Fridlund, A. Gram, H. Jóhannesson, G. Hansson, L. H. Hansson, M. H. Lerche, S. Månsson, R. Servin, M. Thaning, K. Golman, and J. H. Ardenkjær-Larsen, Nucl. Instrum. Methods Phys. Res., Sect. A **526**, 173 (2004).
[53] S. Reynolds and H. Patel, Appl. Magn. Reson. **34**, 495 (2008).
[54] D. Banerjee, D. Shimon, A. Feintuch, S. Vega, and D. Goldfarb, J. Magn. Reson. **230**, 212 (2013).
[55] E. Ravera, D. Shimon, A. Feintuch, D. Goldfarb, S. Vega, A. Flori, C. Luchinat, L. Menichetti, and G. Parigi, Phys. Chem. Chem. Phys. **17**, 26969 (2015).
[56] D. Shimon, Y. Hovav, A. Feintuch, D. Goldfarb, and S. Vega, Phys. Chem. Chem. Phys. **14**, 5729 (2012).
[57] W. T. Wenckebach, Appl. Magn. Reson. **34**, 227 (2008).
[58] Y. Hovav, A. Feintuch, and S. Vega, J. Magn. Reson. **214**, 29 (2012).
[59] S. T. Goertz, Nucl. Instrum. Methods Phys. Res., Sect. A **526**, 28 (2004).
[60] L. Lumata, M. E. Merritt, C. R. Malloy, A. D. Sherry, and Z. Kovacs, J. Phys. Chem. A **116**, 5129 (2012).
[61] C. T. Farrar, D. A. Hall, G. J. Gerfen, S. J. Inati, and R. G. Griffin, J. Chem. Phys. **114**, 4922 (2001).
[62] T. A. Siaw, M. Fehr, A. Lund, A. Latimer, S. A. Walker, D. T. Edwards, and S.-I. Han, Phys. Chem. Chem. Phys. **16**, 18694 (2014).
[63] A. Abragam and B. Bleaney, *Electron Paramagnetic Resonance of Transition Ions* (Oxford University Press, Oxford, 2012).
[64] M. Borghini, Phys. Rev. Lett. **20**, 419 (1968).

[65]J. A. Peters, J. Huskens, and D. J. Raber, Prog. Nucl. Magn. Reson. Spectrosc. **28**, 283 (1996).
[66]K. Nwe, M. Bernardo, C. A. S. Regino, M. Williams, and M. W. Brechbiel, Bioorg. Med. Chem. **18**, 5925 (2010).
[67]N. Chatterton, C. Gateau, M. Mazzanti, J. Pécaut, A. Borel, L. Helm, and A. Merbach, Dalton Trans. **2005**, 1129.
[68]S. C. Serra, M. Filibian, P. Carretta, A. Rosso, and F. Tedoldi, Phys. Chem. Chem. Phys. **16**, 753 (2013).
[69]V. A. Atsarkin, V. V. Demidov, G. A. Vasneva, B. M. Odintsov, R. L. Belford, B. Radüchel, and R. B. Clarkson, J. Phys. Chem. A **105**, 9323 (2001).
[70]B. M. Alsaadi, F. J. C. Rossotti, and R. J. P. Williams, J. Chem. Soc., Dalton Trans. **1980**, 2151.
[71]E. D. T. de Lacheisserie, D. Gignoux, and M. Schlenker, *Magnetism* (Springer Science & Business Media, 2005).
[72]J. Solé, L. Bausa, and D. Jaque, *An Introduction to the Optical Spectroscopy of Inorganic Solids* (Wiley, 2005).
[73]B. R. Patyal, J.-H. Gao, R. F. Williams, J. Roby, B. Saam, B. A. Rockwell, R. J. Thomas, D. J. Stolarski, and P. T. Fox, J. Magn. Reson. **126**, 58 (1997).
[74]H. J. Weinmann, R. C. Brasch, W. R. Press, and G. E. Wesbey, Am. J. Roentgenol. **142**, 619 (1984).